Utilization of waste glass in translucent and photocatalytic concrete

P. Spiesz [a,b,*], S. Rouvas [a], H.J.H. Brouwers [a]

[a] Department of the Built Environment, Eindhoven University of Technology, P.O. Box 513, 5600 MB Eindhoven, The Netherlands
[b] Applied Concrete Research, HeidelbergCement Benelux, ENCI B.V., P.O. Box 1030, NL-3180 AA Rozenburg, The Netherlands

HIGHLIGHTS

- Waste glass is utilized to produce translucent and air purifying concrete.
- Waste glass-based concrete with good mechanical properties and suppressed ASR is developed.
- Air purification ability of concrete is enhanced by the glass particles.

GRAPHICAL ABSTRACT
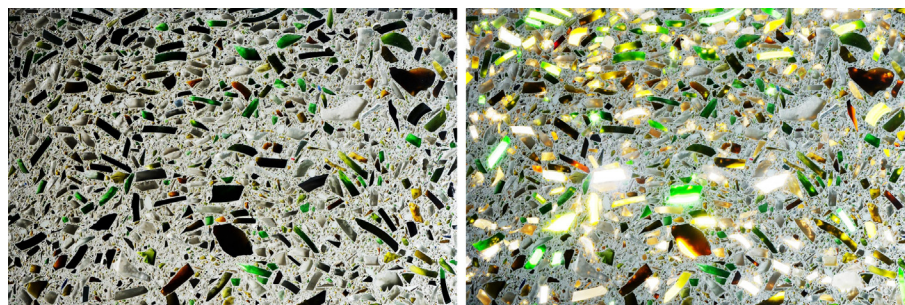
ABSTRACT

This article addresses the development of a translucent and air purifying concrete containing waste glass. The concrete composition was optimized applying the modified Andreasen & Andersen model to obtain a densely packed system of granular ingredients. Both untreated (unwashed) and washed waste glass fractions were utilized in concrete. The fresh and hardened concrete properties were investigated. In order to ensure a durable material, the expansion due to the alkali-silica reaction was also analyzed. Subsequently, concrete tiles of different thicknesses were produced and their translucency was quantified. Additionally, two different types of TiO_2 were utilized in concrete to analyze the glass aggregates effect on the photocatalytic degradation of air pollutants (NO and NO_2). The obtained results indicate that the developed concrete has satisfactory mechanical properties, coupled with good durability, translucency and enhanced air purification properties.

© 2016 Elsevier Ltd. All rights reserved.

1. Introduction

Concrete is the mostly produced manmade material worldwide, reaching about 20–25 Gt of annual production [1]. The architectural possibilities, form flexibility, mechanical properties, durability and relatively low price are the main reasons for its common use. To produce such high amounts of concrete, a high amount of its ingredients is needed, especially fine and coarse aggregates, which in most cases exceed 60% of concrete's volume.

The environmental legislations become increasingly strict over the last decade, new concepts and technologies of materials re-use after their primary service life are being constantly developed (e.g. for recycled concrete [2,3]); therefore the application of recycled or waste materials as concrete ingredients is being strongly promoted. Waste glass can be considered as one of the possibilities. It is a material that cannot be re-used for glass production due to its high chemical pollution and contamination with metal, paper, plastic, porcelain, etc. As a result, waste glass is often either landfilled or disposed in municipal dumping grounds. Furthermore, in most parts of the world the collection and recycling of glass are not well developed. In places where no local glass recycling facilities are available (e.g. Hong Kong [4]) all the collected

---

* Corresponding author at: Department of the Built Environment, Eindhoven University of Technology, P.O. Box 513, 5600 MB Eindhoven, The Netherlands.
E-mail address: przemek.spiesz@heidelbergcement.com (P. Spiesz).

glass is considered a waste material. There are several countries where the consumer packaging glass collection exceeds over 80% of the produced glass (e.g. Germany, Finland, Switzerland, Belgium, the Netherlands, Denmark, Austria, Sweden, Norway [5]) and where a significant majority of this glass is recycled. Nevertheless, even in these countries, the non-recyclable and waste glass constitute a growing problem which needs sustainable and innovative solutions. Therefore, among the possibilities offered by various industry sectors, the utilization of waste glass in building materials can be considered a sustainable solution. Moreover, such a solution can be economically attractive, as it could reduce the demand for conventional raw materials. Investigations on various applications of waste glass in building materials have been widely presented in the literature, e.g. in fired clay bricks [6], paving blocks [7], road applications [8], expanded-glass lightweight aggregates in concrete [9–12], as a binder blended with cement (milled glass) [13–16] or as a raw material in cement production [13,17]. Nevertheless, the waste glass is in most cases used in concrete. It is important to mention here, that majority of the available research considers only washed glass, which unfortunately demands an additional technological step in the concrete production process. Waste glass is available in many different size fractions, from a few micrometers (powder) up to a few centimeters, which makes it possible to replace conventional, mineral concrete aggregates and fillers (fines, sand, gravel) in concrete. As demonstrated in [18,19], broken glass could be used as sand replacement in concrete pavement, asphalt additive and road filler. Moreover, glass aggregate has been also used for the production of aesthetic and decorative concrete [20] because the exposed glass particles in polished surfaces are attractive for certain architectural and decorative applications. In addition to the application of glass aggregates in traditional concrete, research has been also performed on the development of architectural self-compacting concrete (SCC) using fine and coarse glass aggregates [4]. As a result, a decorative concrete (with exposed glass particles) with a complete replacement of conventional aggregates by glass has been produced, having the 28 days compressive strength of 40 MPa.

However, there are some potential issues related to the utilization of glass in concrete. Glass exposed to highly alkaline concrete pore solution is susceptible to alkali-aggregates reaction (AAR) or alkali-silica reaction (ASR), which leads to detrimental expansive ASR products [20–22]. The ASR-damage is a multiple-step, long-term process in which firstly the alkalis originating from cement react with water, producing sodium and potassium hydroxides. Then, the reactive silica present in glass slowly dissolves in the alkaline pore solution. Subsequently, the dissolved silica reacts with the alkali hydroxides, producing a viscous and unstable alkali-silica gel, which is able to imbibe water and swell [22–24]. Additional water enhances the gel development, inducing tensile stresses that lead to a slow concrete deterioration. One way to minimize the ASR risk is to limit the alkali amount in concrete pore solution by using low alkali cements. Suppression and neutralization of the reaction can be also obtained by utilization of pozzolans in concrete [21,23–31]. Pozzolanic materials are characterized by a high silica content and a high specific surface area. Pozzolans consume alkalis to form alkali-silicates, so that no alkalis remain in later stages to react and produce expansive ASR products. In the absence of pozzolanic additives, the reactive silica present in glass particles may slowly dissolve in the alkaline pore solution, react with alkalis and induce the ASR damage. It is important to emphasize that the glass particle size is crucial for ASR, as the glass powder (<300 μm) does not cause ASR issues and can be considered as a pozzolan [16,20,21,32–35], while larger particles are potentially reactive in concrete [36–38].

Besides the ASR risk, other properties of concrete can also be influenced by glass particles. The specific density of glass is lower than that of conventional aggregates, resulting in a decreased density of concrete. Workability and mechanical properties of concrete are also influenced [21,32,33,38–44]. The smooth texture of glass aggregates changes the workability (lower water demand) and reduces the strength of concrete, as the adhesion and interlocking effects between the cement matrix and glass aggregates are weaker than for conventional aggregates. It has been found that a replacement of up to 20% of conventional aggregates with glass does not significantly change the strength of concrete [41–43], whereas for replacement levels higher than 30% the reduction becomes more significant.

The photocatalytic oxidation (PCO) technology is increasingly often applied in building materials to provide them with self-cleaning and/or air-purifying properties. The most commonly used photocatalyst – TiO_2, is proven to perform well in concrete exposed to the outdoor environment. Recently, a full scale demonstration project in Hengelo, the Netherlands, has shown that a significant air pollutants removal (e.g. NO and NO_2, denoted later as NO_x) in the urban environment can be achieved by photocatalytically active concrete [45]. The reported results show that an average NO_x concentration reduction reached over 19% during the entire day length and up to 28% when considering only the afternoons, when the UV-light intensity is the highest. Under the ideal weather conditions the NO_x concentration could be reduced up to 45% compared to the control street paved with standard concrete stones. Besides the UV-active TiO_2 used in outdoor applications, new types of modified TiO_2 (e.g. by doping) that can be activated by the visible light are also becoming widely available. Thus, this type of photocatalyst can be used also in indoor applications. Nevertheless, as TiO_2 is still considered as a relatively expensive additive compared to traditional building materials such as concrete, it is desired to apply it in an optimal and efficient way. As demonstrated in [46,47], one way to minimize the amount of TiO_2 photocatalyst addition in concrete and improve its air purification ability is by a combined application of TiO_2 and glass aggregates. The light transmittance and reflection properties of glass particles are considered the main factors for the PCO efficiency enhancement, as the transferred light could be better scattered across the concrete matrix and activate the TiO_2 particles more efficiently. Therefore, a higher concrete surface at which the PCO oxidation takes place could also play an active role in the process [47].

Combining the sustainability of the application of waste glass together with the aesthetic and functional properties, the aim of the present study is to develop a functional waste glass-based, durable and strong concrete with unique properties: translucency and enhanced air cleaning properties. This is achieved by utilizing waste glass in different size fractions and TiO_2 photocatalyst to produce concrete tiles of various thicknesses. As the currently available literature investigates mainly the application of washed glass in concrete, this article targets also on concrete prepared with unwashed waste glass.

2. Materials

The waste glass used in this study originates from a glass recycling company (Maltha Glasrecycling Nederland B.V.) and has particles in the size range of 20 μm up to 14 mm. In total, five different glass fractions are used, as illustrated in Fig. 1. The received glass is considered a waste material due to its high chemical pollution and contamination that are too high for recycling in glass production factories. Prior to the delivery, it has been screened to different size fractions and stockpiled in natural weather conditions. In this study, the fine and coarse waste glass aggregates are firstly applied in concrete in their original, polluted form. This pollution mainly includes decomposed organics (sugar, fat, etc.) and soil. Due to the detrimental influence of the pollution on concrete properties,
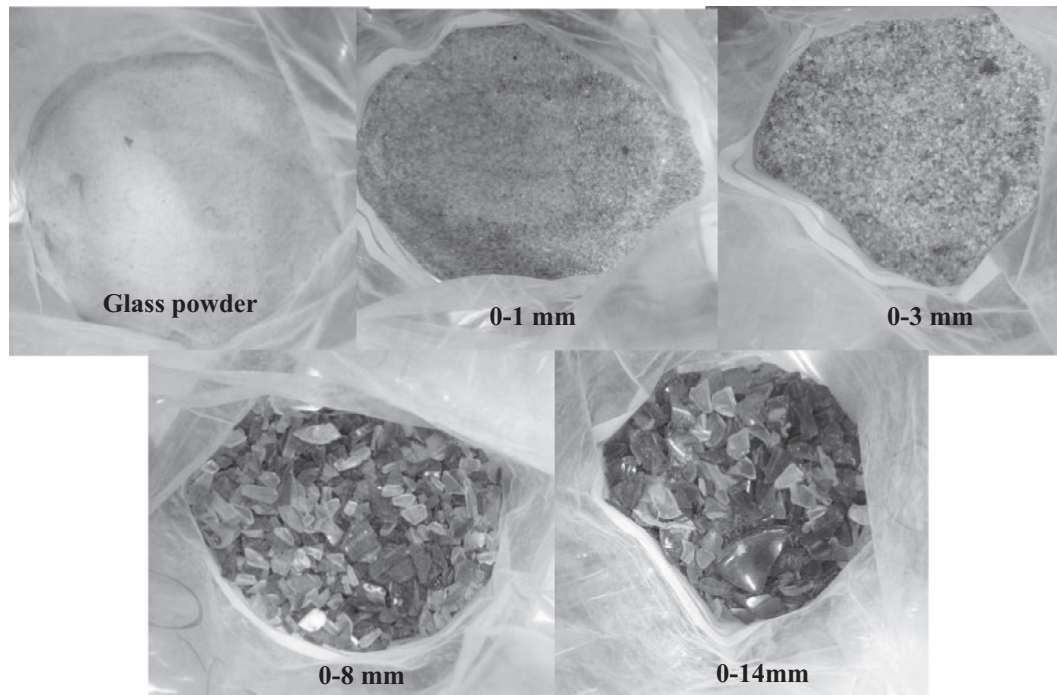
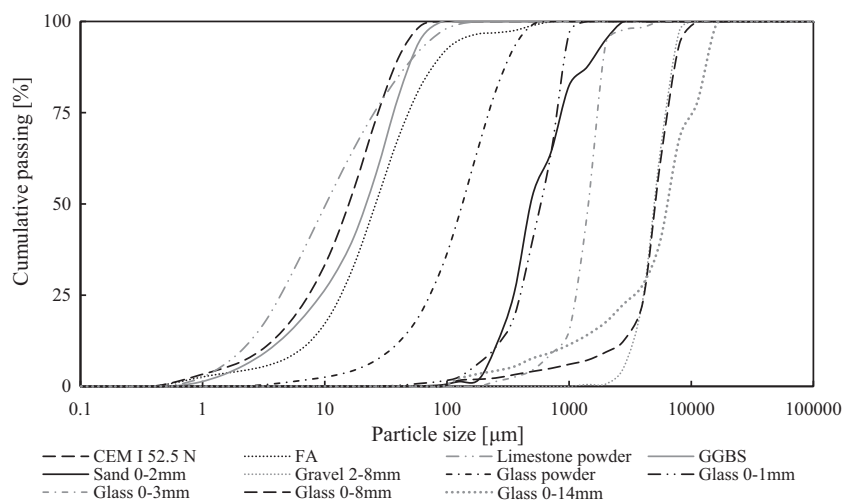**Fig. 1.** Waste glass fractions used in this study.

Fig. 2. Particle size distribution of powders and aggregates.

also washed glass fractions are used. The cement used in this research – CEM I 52.5 N – white, is a low-alkali cement (< 0.60%), supplied by HeidelbergCement Benelux. The conventional aggregates comprise of a river dredged sand (0–2 mm) and broken gravel (2–8 mm) and limestone powder is used as a fine filler. Two pozzolanic materials (ground granulated blast-furnace slag and fly ash) are also utilized as binders and ASR suppressors. The particle size distributions of the used granular materials are presented in Fig. 2. In order to adjust the flowability of fresh concrete mixtures a polycarboxylate superplasticizer (SP) is used. Two different types of TiO$_2$ photocatalysts are applied in this study to provide the concrete with air purifying and self-cleaning properties: Aerodisp W 740 X (Evonik, Germany) is a water-based dispersion of fumed TiO$_2$ and Krono Clean 7404 (Kronos, Germany) is a carbon-doped TiO$_2$, also in a slurry form. The properties of both TiO$_2$ additives are summarized in Table 1.

Table 1
Properties of the used TiO$_2$ additives.

Product name	AERODISP W 740 X	KRONO Clean 7404
TiO$_2$ type	Anatase	Anatase
TiO$_2$ content in slurry	40%	40–50%
pH	6.0–9.0	7.0–8.0
Viscosity	⩽1000 mPas	⩽800 mPas
Density (slurry)	1.43 g/cm^3	1.40 g/cm^3
Appearance	Milky liquid	Brownish liquid
Particle size	40–300 nm	10–200 nm

3. Test methods

3.1. Compressive and flexural strength test

The mechanical properties of the developed mixtures are determined following EN 196-1 [48]. A set of nine prisms

$(40 \times 40 \times 160 \text{ mm}^3)$ is cast per each mixture. Immediately after casting, the concrete is poured into molds and covered to prevent from drying. After a period of 1–3 days (depending on the hardening of concrete) the prisms are demolded and stored in water (20 °C). The 1 day strength was not possible to be determined for some mixtures, as the setting time was significantly delayed by the polluted unwashed glass. Therefore, the strength measurements are performed at 1–3 days (depending on the mixture), 7 and 28 days after casting.

3.2. Alkali-silica reaction (ASR) test

The accelerated ASR test procedure as described in ASTM C1260-01 [49] and RILEM TC 106-AAR guideline [50] is followed. Only the concrete compositions developed in this study are investigated, thus not the compositions specified in [49]. One day after casting the prisms ($40 \times 40 \times 160 \text{ mm}^3$ with embedded stainless-steel pins for the length measurements), they are demolded and stored for an additional one day in hot water (80 °C). After that, the initial length of the samples is measured (L_0) with an apparatus capable to measure the expansion in a μm-scale, and subsequently the samples are subjected to 1 N NaOH solution in an oven at 80 °C. The expansion is measured periodically. The total cumulative expansion (E) is calculated as the difference between the final length of the prism L_n after storing for 14 days in the NaOH solution and the initial length L_0, divided by the gauge length of the cast prism L_i (160 mm), as shown in Eq. (1):

$$E\,[\%] = \frac{L_n - L_0}{L_i} \cdot 100\%$$

(1)

3.3. Translucency

In order to produce translucent concrete samples, concrete beams ($150 \times 150 \times 400 \text{ mm}^3$) are firstly cast, demolded after 1 day and cured in water (20 °C) for 28 days. Subsequently, the hardened beams are cut to slices (tiles) using a precision diamond saw. Tiles of $150 \times 150 \text{ mm}^2$ and different thicknesses are produced for the translucency measurements. A light luminance meter is used to determine the translucency. The device is connected to a sensor placed in a sealed wooden box, as presented in Fig. 3. The intensity of the lighting source (outdoor conditions, sunny weather, clear sky) is firstly measured by the sensor placed in the uncovered box, yielding about $1 \cdot 10^5$ lx. Subsequently, the concrete tile is placed on top of the box, closing it firmly, and then the light intensity inside the box is measured. Multiple measurements are taken on both sides of each sample for a better results reliability.

3.4. Photocatalytic oxidation of air pollutants

For the photocatalytic oxidation (PCO) tests, two tiles (dimensions of $100 \times 200 \times 20 \text{ mm}^3$) are cast for each developed mixture. One day after casting, the samples are demolded and cured in water until the age of 28 days. Subsequently, the top surfaces of the plates are polished using a wet grinding device, in order to expose the embedded aggregates, and dried in an oven. Finally, the PCO experiments are performed following the ISO 22197-1:2007 [51]. Fig. 4a shows a concrete tile mounted in the reactor prior to the PCO experiments. After inserting the sample, the

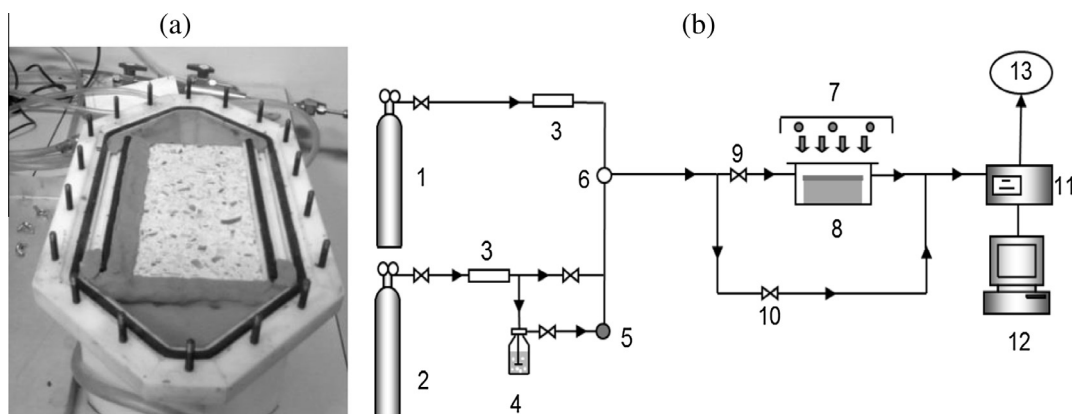
Fig. 3. Translucency measurement test set-up.

Fig. 4. (a) concrete sample mounted in the reactor and (b) PCO measurement test set-up.

reactor is tightly sealed with a transparent borosilicate glass plate. Then, the reactor is connected to the PCO test set-up and the pollutant (NO) is mixed with synthetic air to get an initial concentration of 1 ppm and a volumetric flow rate of 3 L/min. After reaching stable conditions inside the reactor, the concrete sample is exposed to the irradiating light. The applied light source consists of three cool ultraviolet lamps of 25 W each, emitting an ultraviolet radiation (UV) in the range of 300–400 nm. The light intensity is measured with an UVA radiometer. A schematic diagram of the PCO set-up is presented in Fig. 4b [52]. The experiments are performed at room temperature (20 °C). The air stream is humidified by flowing into a bottle filled with demineralized water, to ensure a steady 50% relative humidity during the measurements. The pollutant concentration is adjusted by mass control meters to reach the appropriate proportions of the gases. The PCO reaction takes place immediately once the sample is exposed to the UV-light. The stream of the outlet reactor gas is directed to the NO_x concentration analyzer, where the outlet concentration of air pollutants is measured (including the unreacted NO and generated NO_2). To determine the efficiency of the pollutant degradation (conversion), the difference between the inlet and outlet pollutant concentrations in the reactor is determined, taking into the account also the NO_2 concentration. Two samples are tested for each developed concrete composite and an average PCO conversion of NO_x is then computed.

4. Concrete design

All mixes developed in this study are self-compacting concretes (SCC), i.e. having a very high flowability and self-densification properties. For the mix design, an algorithm based on the modified Andreasen & Andersen (A&A) particle packing model is employed [53]. This method has been already used to develop many different types of concrete, including SCC [54–56], zero-slump [53,57], normal [54], lightweight [9–12] or high-performance [58,59] and gypsum-based composites [60]. An optimized packing results in a denser structure with minimized voids content, which in turn improves workability (fresh state) and mechanical properties (hardened state). The modified A&A model reads as follows [54,61]:

$$P(D) = \frac{D^q - D_{min}^q}{D_{max}^q - D_{min}^q} \ \forall \ D \in [D_{min}, D_{max}] \tag{2}$$

where $P(D)$ – the cumulative passing fraction through a sieve with an opening of D [μm], D_{min} and D_{max} – the minimum and maximum

particle size of the used materials [μm] and q – the distribution modulus, which determines the proportion between the fine and the coarse particles in the mixture.

In this study, a distribution modulus of 0.23 is adopted based on the recommendations given in [55] for SCC. Firstly, a target grading curve is computed using Eq. (2) and then the mixture grading curve is optimized in order to obtain a close fit to the target. Fig. 5 shows as an example the optimized and target grading curves for the reference concrete mixture. The water/binder ratio of the mixtures is fixed at 0.39 for the mixtures with unwashed glass particles and 0.33–0.40 for the mixtures with washed glass. The flowability of concrete mixtures is adjusted by adding superplasticizer, up to a maximum dosage of 2% by mass of cement. In this study, a target spread flow (measured following EN 1015-3 [62]) holds in the range of 190–230 mm using a Hägermann cone. The recipes of all the optimized SCC mixtures are given in Table 2. The reference SCC mixture is prepared using conventional sand and coarse aggregates, and cement and fly ash (FA) as binders. Glass-based SCC mixtures are developed in two series. Series 1 investigates the properties of SCC based on unwashed, "as received" glass fractions (Mixes 1 and 2). Here, the water has been increased to comply with the target flowability, as the glass pollution caused a strong flowability reduction. Moreover, in Series 1 the influence of individual glass fractions (powder, sand and coarse aggregates) on concrete properties are investigated by replacing only one mineral ingredient (Mixes 3–5). Thus, in Mix 3 gravel 2–8 mm is replaced by glass aggregates 0–8 mm; in Mix 4 limestone powder is replaced with glass powder and in Mix 5 sand 0–2 mm is replaced with glass sand. The granular composition of these mixtures was further optimized following Eq. (2) to obtain a denser packing, maintaining only the cement and FA amounts constant for a comparison with the reference. Series 2 focuses on the development of concrete suitable for production of translucent tiles in concrete prefab industry. In order to limit the significant flowability decrease and strongly extended setting time caused by the pollution in glass, only washed glass was used here. Due to technical complexity of washing and drying the polluted glass powder, this fraction has not been applied in the mixtures. In this series, a complete replacement of all the fine and coarse aggregates with waste glass particles is done to utilize the highest amount of waste glass. The focus of Series 2 is to develop SCC mixtures having high glass content for better translucency effects, white color (aesthetic reasons), satisfactory mechanical properties and no ASR-damage risk. Therefore, waste glass is washed and dried, higher binder dosages are used to ensure better mechanical properties and a white ground granulated blast-furnace slag (GGBS) is used instead of
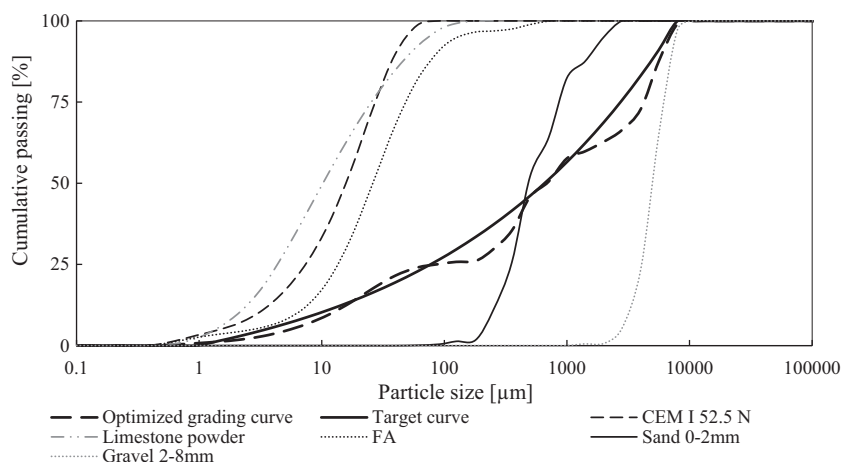

Fig. 5. Target and optimized grading curves for the reference concrete mixture.

Table 2
SCC mix proportions.

Series	Mix	Mixture proportions [kg/m^3]											
		Water	Binders			Aggregates and filler			Glass aggregates and filler				
			CEM I 52.5 N white	FA	GGBS	Limestone powder	Sand 0–2 mm	Gravel 2–8 mm	Glass powder	0–1 mm	0–3 mm	0–8 mm	0–14 mm
Reference	Ref	180	360	100	–	115	813	735	–	–	–	–	–
Series 1	1	252	360	100	–	–	–	–	99	265	106	782	–
	2	342	360	–	–	–	–	–	287	83	82	828	–
	3	180	360	100	–	111	813	–	–	–	–	708	–
	4	180	360	100	–	–	663	732	252	–	–	–	–
	5	180	360	100	–	111	–	740	–	664	104	–	–
Series 2	6	200	400	–	105	–	–	–	–	458	186	–	873
	7	182	400	–	100	150	–	–	–	285	332	–	811
	8	182	400	30	70	150	–	–	–	285	328	–	808
	9	182	400	–	151	102	–	–	–	320	297	568	300*

* Only sieved fraction >8 mm used.

Table 3
Concrete mix proportions for the PCO tests.

Control SCC Dosage [kg/m^3]	CEM I 52.5 N 460.8	Limestone powder 132.9	Sand 0–2 mm 813.5	Gravel 2–8 mm 734.6	Water 206.9
SCC with glass Dosage [kg/m^3]	CEM I 52.5 N 460.8	Limestone powder 132.9	Glass 0–3 mm 770.7	Glass 0–8 mm 703.7	Water 206.9

fly ash to preserve the material's white color. Mix 6 developed in Series 2 is composed of a binder (CEM I + GGBS) and waste glass aggregates only, whereas in Mix 7 the powder content is increased by adding limestone powder for improving the mixture grading. In order to investigate the GGBS and FA efficiency on reducing the ASR damage, in Mix 8 part of the GGBS is replaced with FA. Mix 9 comprises of an increased amount of coarse glass aggregates (> 8 mm) to study the effect of large glass aggregates on the translucency of concrete.

Twelve different mixtures are prepared in this study for the air pollutants photocatalytic oxidation (PCO) tests of concrete – six reference and six mixtures with waste glass. The basic recipes for the Control and waste glass concrete are given in Table 3. The Control concrete comprises of conventional aggregates, while the waste glass concrete is prepared with fine and coarse waste glass aggregates. The TiO$_2$ photocatalyst is added to the mixtures by replacing an equivalent volume of limestone powder, at the dosages of 3, 5 and 7% by the mass of cement. As mentioned earlier, two different TiO$_2$ types are investigated in this study to analyze their effect. Water present in the TiO$_2$ slurry is subtracted from the total mixing water amount.

5. Results and discussion

5.1. Compressive and flexural strengths

Fig. 6 presents the mechanical properties development of Series 1 samples, in which unwashed waste glass was applied. It can be found that both the compressive (Fig. 6a) and flexural (Fig. 6b) strengths of the reference concrete (no waste glass additions) are the highest among all the developed mixtures. The 1 day strength of the mixtures containing unwashed glass was not possible to be determined, as the pollution of glass distorted the cement hydration and significantly delayed the setting time. Therefore, for Mixes 1, 2 and 5 only the 3 days strengths were determined and for Mixes 3 and 4 the early age strength tests were skipped altogether. The strength of mixtures prepared with a complete replacement of

conventional aggregates by glass (Mixes 1 and 2) are very low compared to the reference mixture. In the case of Mix 1, the 28 days compressive strength reached only about 22 MPa compared to about 60 MPa for the reference SCC. Even more pronounced strength reduction is observed for Mix 2 (only about 13 MPa compressive strength), in which fly ash is replaced by glass powder. Such low mechanical properties of concrete with waste glass can be attributed mainly to the pollution introduced into the concrete by the unwashed glass. Also the water content (i.e. water/binder ratio) in these mixtures is significantly increased to maintain the flowability requirements, as the maximum recommended dosage of superplasticizer (2% by mass of cement) was insufficient. Therefore, it can be concluded that a complete replacement of traditional concrete aggregates and fillers with unwashed waste glass is very detrimental to concrete mechanical properties. The influence of individual glass fractions on the properties of concrete can be observed in Fig. 6 for Mixes 3–5. Mix 3, in which only gravel 2–8 mm has been replaced by 0–8 mm unwashed glass particles shows a delayed setting (early age strength was not determined) and a reduction of both the compressive and flexural strengths of about 30% compared to those of reference concrete. A slightly lower reduction (about 25%) is observed for the mixtures where either limestone powder or sand 0–2 mm are replaced with unwashed glass powder or sand (fractions 0–1 and 0–3 mm), respectively. Therefore, it can be concluded that the investigated fractions of unwashed waste glass individually are detrimental to the mechanical properties of concrete in a similar manner. Moreover, washing the waste glass seems an inevitable treatment to minimize the negative influence of pollution on the properties of concrete. Based on these observations, in Series 2, concrete mixtures are based on washed and dried glass fractions. Waste glass powder is not used here due to its high pollution related to the high specific surface area and difficulties with proper washing. The compressive and flexural strength developments of Mixes 6–9 are presented in Fig. 7. Mix 6 is developed with a lower amount of powders (no limestone powder and glass powder used). The decreased powder content in Mix 6 results in a worse packing density of the granular matrix (higher void fraction) and, as can be
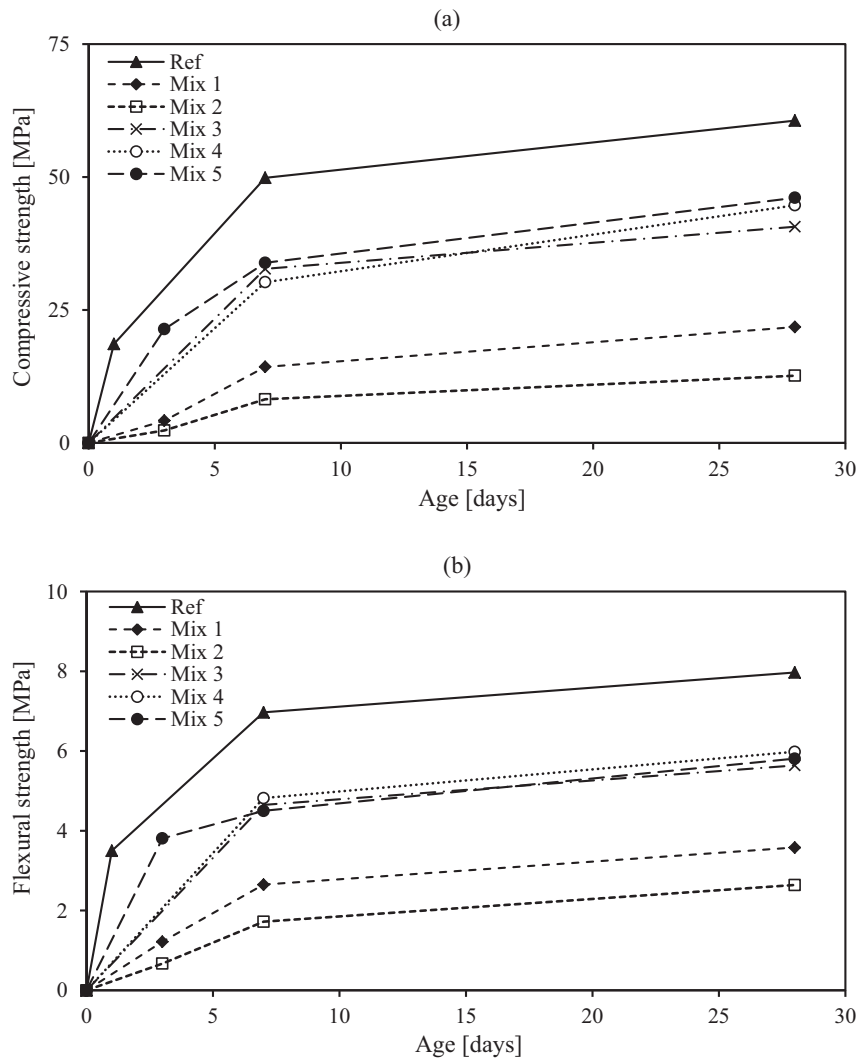
(a)

(b)

Fig. 6. (a) compressive and (b) flexural strengths development of concrete (Series 1, Mixes 1–5).

observed in Fig. 7, in reduced mechanical properties compared to the other mixtures (about 50% lower strength compared to the reference concrete). Therefore, to improve the mechanical properties, limestone powder is utilized as a fine filler and the water/binder ratio is slightly reduced in Mixes 7–9. As can be observed in Fig. 7a, the 28 days compressive strength of Mix 7 reaches about 45 MPa and about 42 MPa for Mixes 8 and 9.

In order to further analyze the influence of the waste glass on the mechanical properties of concrete, the binder efficiency is estimated here. A binder efficiency is expressed as the ratio between the 28 days compressive strength and the total amount of binder (CEM I, GGBS and FA) used to produce 1 m^3 of concrete [55]. Table 4 presents a summary of the concrete compositions developed in this study including the compressive strength, binder dosage, total glass content and binder efficiency. Fig. 8 presents the binder efficiency computed for all the mixtures developed in this study vs. the total utilized glass content. The binder efficiency of about 0.13 is obtained for the reference concrete, which is in agreement with values presented by Hunger [55] for SCC with limestone powder additions. It is evident that the glass content and type (washed/unwashed) strongly influences the binder efficiency. For low total glass contents in concrete (10–30 vol%), the binder efficiency is reduced by about 30% compared to the reference concrete. It can be observed in Fig. 8 that the unwashed waste glass powder

reduces the binder efficiency much more than the sand and coarse waste glass aggregates, as the glass powder content in Mix 4 was only about 10 vol% and the binder efficiency in this mixture is similar to Mixes 3 and 5, where the fine and coarse glass aggregates content is about 30 vol%. Comparing the data shown in Fig. 8 for mixtures completely based on the waste glass (without conventional gravel/sand), it can be seen that washing the glass increases the binder efficiency from about 0.04 (Mixes 1 and 2) to 0.06–0.09 (Mixes 7–9). Concrete mixtures with about 60 vol% of washed glass show similar binder efficiencies as the mixtures with only 10–30 vol% of unwashed glass.

5.2. ASR

The accelerated ASR expansion test results are shown in Fig. 9a for Series 1 (concrete with unwashed waste glass) and in Fig. 9b for the Series 2 (concrete with washed waste glass). The criterion given in ASTM C1260 [49] for a maximum allowed expansion of 0.1% after 14 days exposure to 1 N NaOH solution at 80 °C is not considered in this study for the assessment of the ASR risk in the developed mixtures, as this value refers only to mortars prepared with the compositions defined in [49]. Therefore, the investigated concretes containing waste glass are compared in this study only to the reference mixture, in which conventional aggregates were
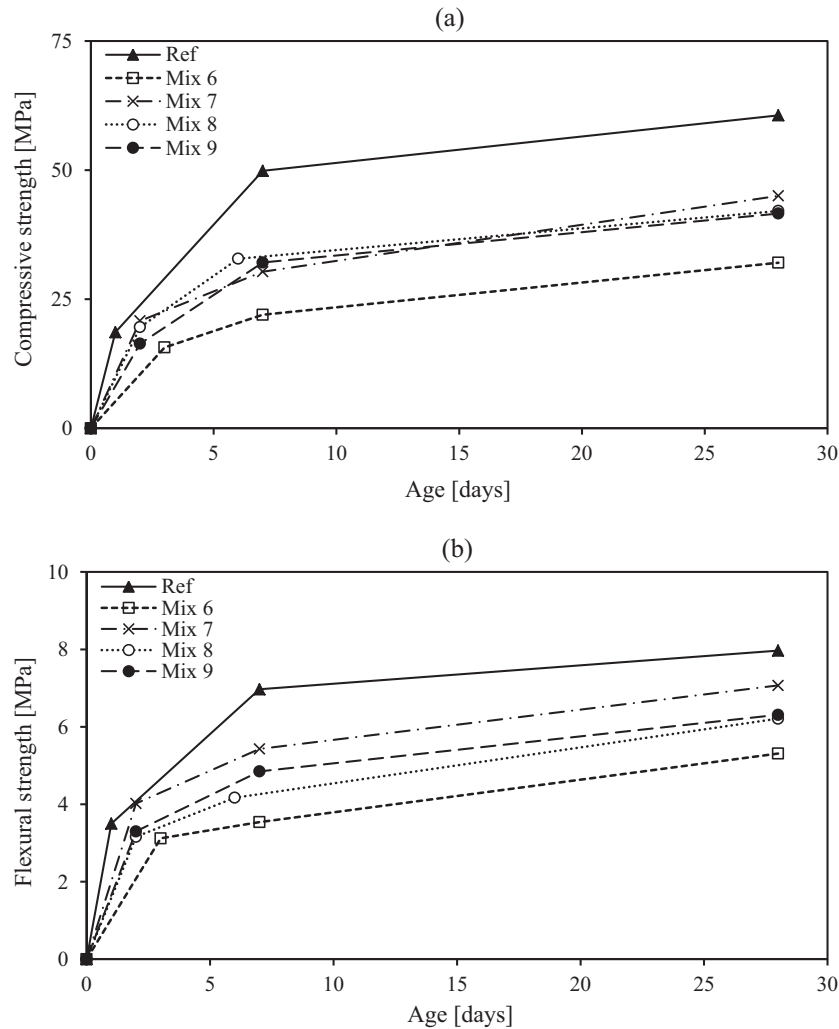
(a)

(b)

Fig. 7. (a) compressive and (b) flexural strengths development of concrete (Series 2, Mixes 6–9).

Table 4
Properties of the developed SCC mixtures.

Mixture	Compressive strength at 28 days [MPa]	CEM I 52.5.N [kg/m³]	FA [kg/m³]	GGBS [kg/m³]	Total binder [kg/m³]	Water [kg/m³]	w/b -	Total glass content [vol%]	Binder efficiency [MPa/(kg/m³)]
Reference	60.6	360	100	0	460	180	0.39	0.00	0.132
Mix 1	21.8	360	100	0	460	252	0.55	55.60	0.047
Mix 2	12.6	360	0	0	360	342	0.95	51.15	0.035
Mix 3	40.7	360	100	0	460	180	0.39	28.20	0.088
Mix 4	44.7	360	100	0	460	180	0.39	10.10	0.097
Mix 5	46.1	360	100	0	460	180	0.39	30.70	0.100
Mix 6	32.1	400	0	105	505	200	0.40	60.50	0.064
Mix 7	45.0	400	0	100	500	182	0.36	56.90	0.090
Mix 8	42.1	400	30	70	500	182	0.36	56.60	0.084
Mix 9	41.6	400	0	151	551	182	0.33	56.10	0.075

used. In the case of the reference mixture, a low expansion of about 0.037% can be observed in Fig. 9a and b, and this can be explained by the absence of a reactive silica source in the applied conventional sand and aggregates. It can be seen in Fig. 9a that the expansion of Mixes 1–5 is low, and comparable to the reference samples. The highest expansion observed in Fig. 9a is for Mix 3, in which only the coarse aggregates were replaced with coarse waste glass particles. This is in line with [36,37], who found that ASR-induced expansion is higher for larger glass particles. The presence of reactive silica in glass applied in Mixes 1–5 does not result in

their significant expansions, and this could be explained by the application of fly ash (FA) and glass powder in these mixtures. It is known from the literature that the glass powder has a positive effect on limiting the ASR [16]. Nevertheless, as there was no glass powder applied in Mixes 3 and 5 and their expansions are in the same order of magnitude as for the other compositions, no beneficial effect of the glass powder on the ASR limitation beyond the effect of FA can be concluded here. However, it can be observed from the experimental results presented in this study that fly ash is as an efficient ASR suppressor. It is known that FA reduces the
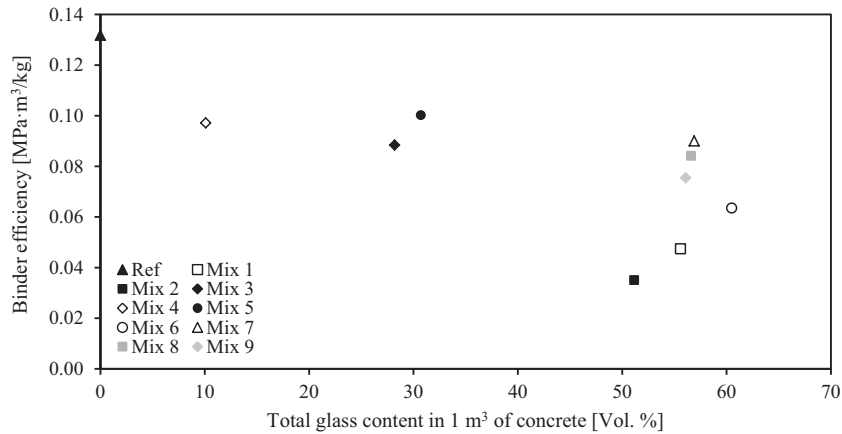
Fig. 8. Binder efficiency at different waste glass contents in concrete.
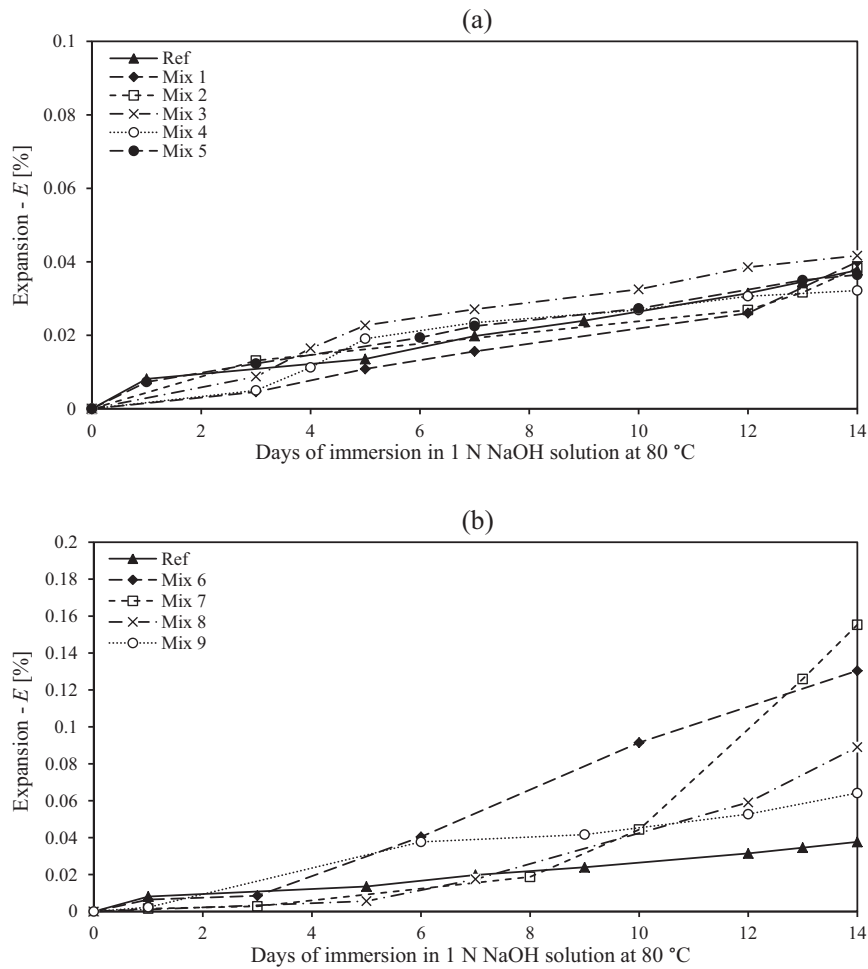

Fig. 9. ASR expansion of concrete – (a) Series 1 (Mixes 1–5) and (b) Series 2 (Mixes 6–9).

alkali concentration in the pore solution of concrete and consumes Ca(OH)$_2$ through the pozzolanic reaction [63,64]. Du and Tan [23] demonstrated that FA is the most efficient ASR suppressor among a number of mineral additives tested, followed by ground granulated blast-furnace slag (GGBS). As suggested by [26,65], ASR can take place only at sufficient Ca^{2+} concentrations in the pore solution, even in the presence of alkalis. Although FA is confirmed to be an effective ASR suppressor, it has not been used in Series 2 of

concrete mixtures developed in this study, as it gives the hardened concrete a grey coloration. Therefore, in Mixes 6–9, a white GGBS has been applied as an ASR suppressor. A small addition of FA was utilized only in Mix 8 to analyze the effect of combined FA and GGBS on ASR. The ASR test results for Mixes 6–9 are presented in Fig. 9b. It can be noticed that all the concrete mixtures prepared with washed waste glass particles show expansions higher than the reference concrete (without glass). The greatest
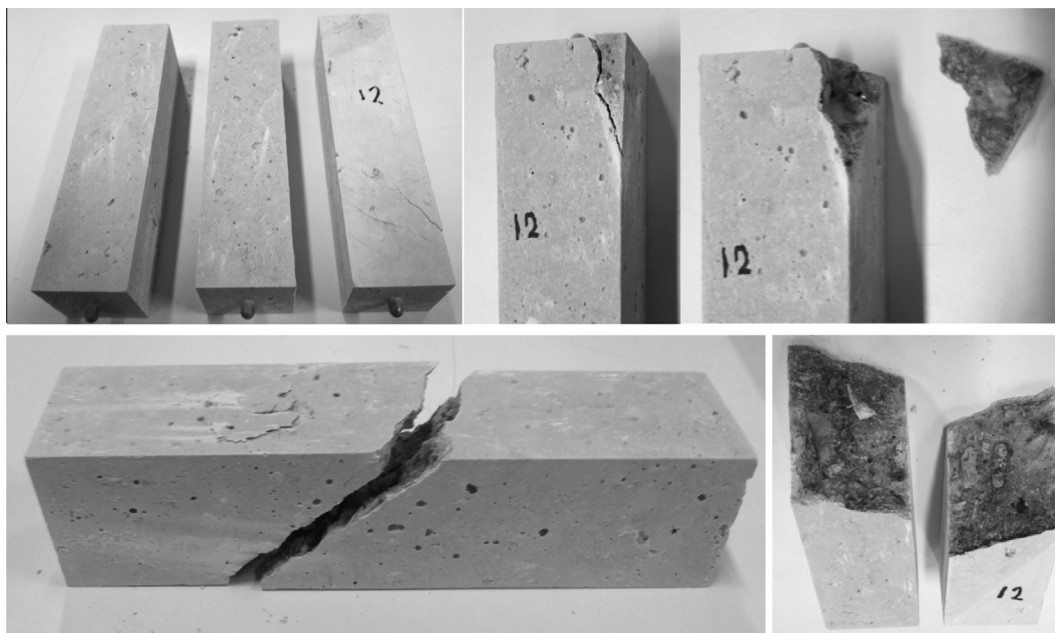
Fig. 10. ASR-induced damage of concrete samples.

ASR-expansion is observed here for Mixes 6 and 7 (3–4 times higher than that of the reference concrete), which reflects that there could be a risk of ASR damage in these mixtures. Fig. 10 shows samples of Mixes 6 and 7 with clear cracks and spalling caused by ASR. The binder in these mixtures is composed of 80% ordinary Portland cement (OPC) and 20% GGBS, thus it can be concluded that such dosage of GGBS is insufficient to effectively limit the ASR expansion. On the other hand, Mix 9 with the binder blend composed of 72% OPC and 28% GGBS shows that the ASR expansion is significantly reduced. Therefore, the results suggest that there is a minimum amount of GGBS in blends with OPC that can mitigate the ASR risk. The binder composition in this mix is similar to CEM II/B-S cement composition, and hence, it can be concluded that by applying this type of cement or CEM III, should also result in ASR suppression. The binder in Mix 8 composed of 80% OPC, 14% GGBS and 6% FA displays an expansion much lower than measured for Mix 7 (similar composition, except for a higher GGBS content and no FA). This result reflects again that FA is a very efficient ASR suppressor.
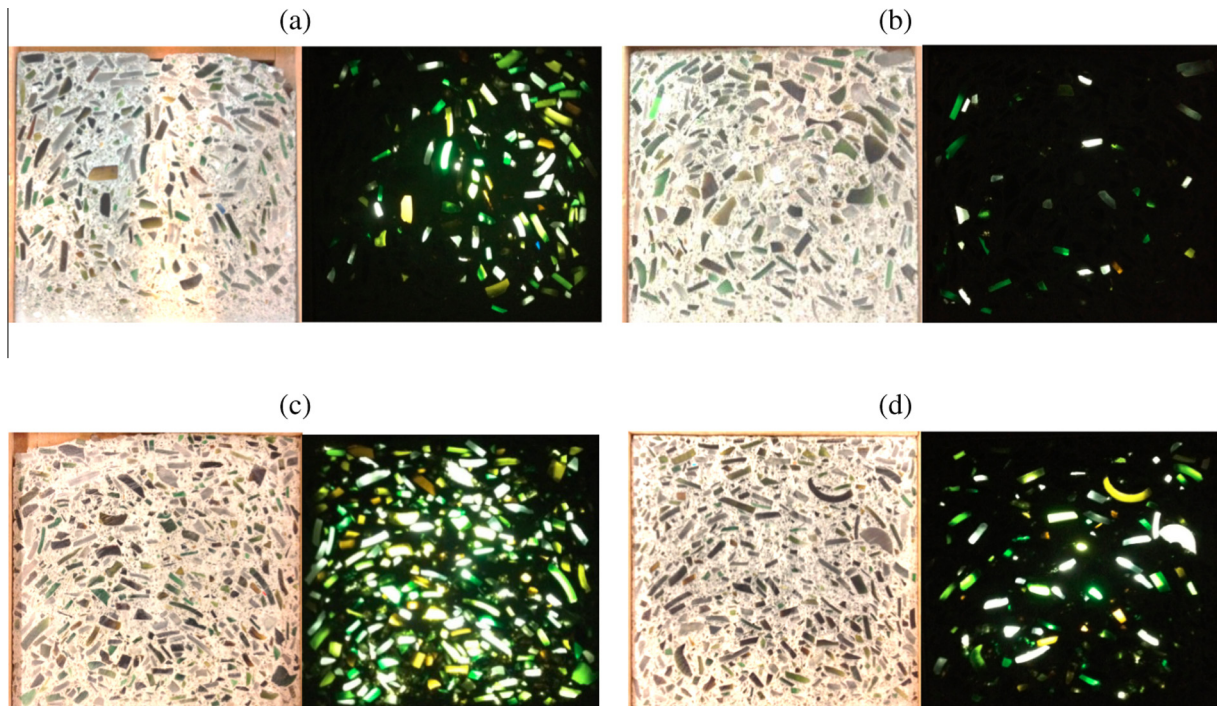
5.3. Translucency

The concrete mixtures analyzed for the light translucency are selected based on the strength and ASR test results presented in the previous sections. As a research target, the desired mixtures should have sufficient mechanical properties, no risk of ASR, high content of waste glass for a higher translucency effect and white color (aesthetic reasons). Two mixtures developed in the Series 2 fulfill these requirements, namely Mixes 8 and 9, and therefore the concrete samples for the translucency tests are prepared with these mixtures. The test tiles are cut to different thicknesses to analyze their influence on the translucency, which in this study is expressed as the % ratio between the luminance of the light passing through the concrete tile and the luminance of the lighting source. Some selected pictures of the test plates are shown in Fig. 11, using an artificial light source (photo camera flash). The measured translucency values for the samples prepared with Mix 8 as a function of different tile thicknesses are presented in Fig. 12a. It can be observed that the translucency increases with a decreasing sample thickness, i.e. more light is able to penetrate

through thinner samples. This effect results from the fact that the visible light is able to penetrate only through those glass particles, which are exposed on both sides of the tile, and not through the hardened cement paste. Therefore, with a decreasing tile thickness, the number of single glass aggregates exposed on both sides of the tile increases, which yields a higher translucency. As the maximum aggregate size used in this study is about 14 mm, this thickness can be considered as the maximum to obtain any translucency. Nevertheless, as the amount of coarse particles is limited (only about 1/3 of 0–14 mm coarse glass aggregates are larger than 8 cm, see Fig. 2) the translucency of tiles thicker than 8 mm is also very low. Fig. 12b presents the translucency of tiles prepared with Mix 9, in which an increased amount of coarse glass aggregates (>8 mm) was used. As expected, the translucency measured for this mixture was significantly higher than for Mix 8. It can be observed that the translucency of a 10 mm thick tile of Mix 9 was comparable with that of a 5 mm thick tile of Mix 8. However, for the tiles thicker than about 11 mm, the measured translucencies are at a low levels. Additionally, it can be observed from the translucency measurement results that the total glass aggregate content in concrete influences the translucency less significantly than the coarse glass aggregates content, because the total glass content in Mixes 8 and 9 was similar (about 56 vol%, see Table 4). Therefore, it can be concluded that the translucency of concrete tiles strongly depends upon their thicknesses, maximum glass aggregate size and its content in concrete. As only the coarsest aggregates contribute to a higher translucency, the maximum glass aggregate size should be increased in order to increase the tile thickness.

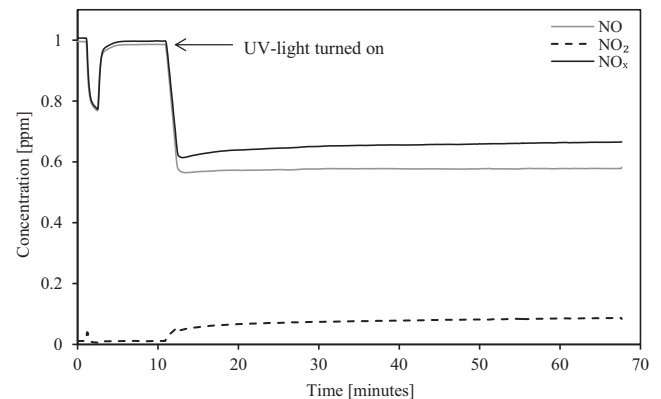### 5.4. Photocatalytic air pollutant oxidation

Fig. 13 presents the nitrogen oxides concentration development in the reactor due to the photocatalytic oxidation (PCO) reaction for the Control SCC with a 5% addition of TiO_2 AERODISP W 740 X. It can be observed that the PCO reaction is responsible for a significant reduction of the nitrogen oxide concentration in the flowing gas stream. The photocatalytic oxidation begins immediately when the concrete sample is exposed to the UV-light, as shown in Fig. 13. After switching on the UV-light source, the source

Fig. 11. Translucent concrete plates of different thicknesses: (a) Mix 8 – 4 mm, (b) Mix 8 – 8 mm, (c) Mix 9 – 4 mm and (d) Mix 9 – 8 mm.
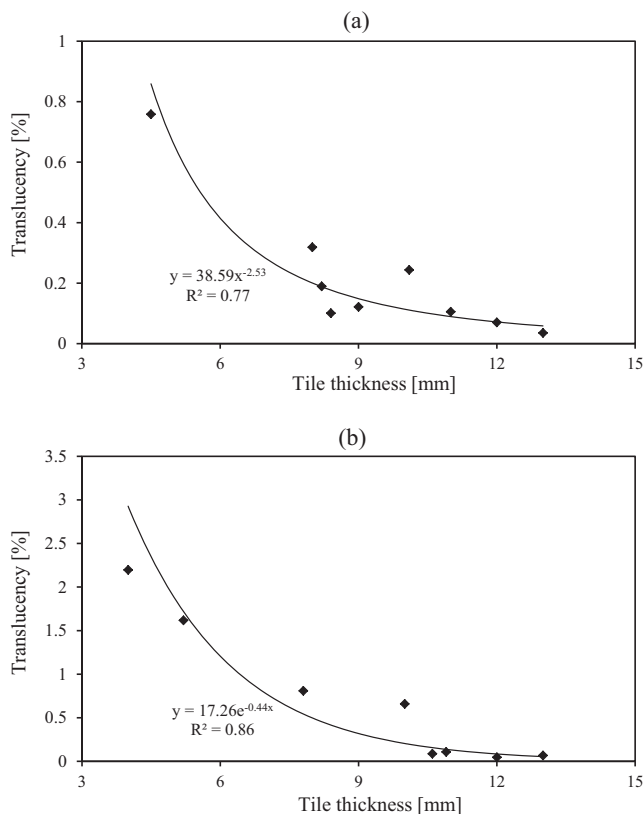
Fig. 12. Translucency at different tile thickness, (a) Mix 8 and (b) Mix 9.

Fig. 13. NO_x concentrations development during the PCO test.

pollutant (NO) is oxidized to nitric ions. However, it can be observed that the NO_2 concentration increases in the reactor outlet gas as NO_2 is an intermediate oxidation product, which is not completely oxidized to nitric ions. The PCO removal (conversion)
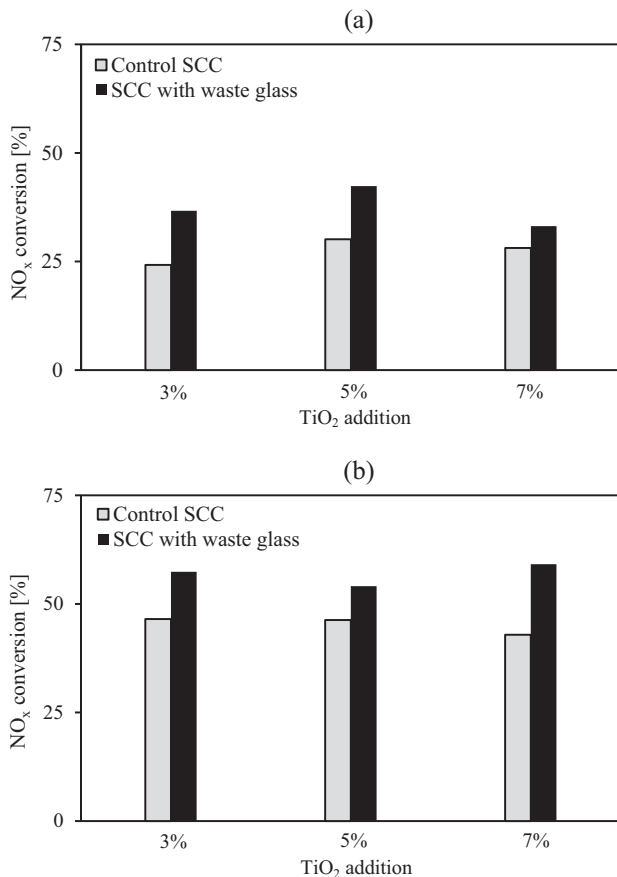
efficiency of air pollutant is calculated including the total NO and NO_2 concentrations (denoted as NO_x), as follows [52]:

$$NO_{x\_con} \ [\%] = \frac{[NO_x]_{in} - [NO_x]_{out}}{[NO_x]_{in}} \cdot 100 \ [\%] \tag{3}$$

where NO_{x_con} – NO_x conversion efficiency, $[NO_x]_{in}$ – inlet NO_x concentration and $[NO_x]_{out}$ – outlet NO_x concentration.

Fig. 14a presents the average NO_x conversion efficiencies of the developed SCC Control and waste glass samples with Evonik AERO-DISP W 740 X TiO_2 photocatalyst. For the Control SCC samples, the conversion efficiencies hold in the range of 20–30%. The NO_x conversion efficiency in the samples containing glass aggregates is significantly improved, especially in the samples containing 3 and 5% TiO_2 additions (52 and 41% higher conversion than the Control samples, respectively). Fig. 14b presents the NO_x conversion efficiency of the SCC Control and waste glass samples with KRONO Clean 7404 TiO_2 photocatalyst. Again, a noteworthy NO_x conversion improvement can be observed for the samples containing waste glass particles (17–38% improvement). Hence, it can be

Fig. 14. NO$_x$ conversion efficiency of SCC with different additions of TiO$_2$ – (a) AERODISP W 740 X and (b) KRONO Clean 7404.

concluded that glass particles, due to their light transmittance and scattering properties, can enhance the TiO$_2$ activation by the UV-light, so that the TiO$_2$ photocatalyst can be better utilized in concrete, yielding higher air pollution removal efficiency.

Analyzing the results shown in Fig. 14, it can be noticed that there is no significant NO$_x$ conversion efficiency improvement for the TiO$_2$ dosages exceeding 3% addition by the mass of cement. A possible explanation for this phenomenon is the experimental conditions (e.g. the air flow rate through the reactor), which can limit the amount of the NO$_x$ and H$_2$O molecules adsorbed on the TiO$_2$ active surface [52,66], i.e. limit the maximum number of NO$_x$ molecules that could be oxidized. Therefore, even for an increased number of TiO$_2$ particles in the system, the total PCO efficiency could remain at similar levels. It can be concluded that the presented results show that an optimum TiO$_2$ addition of 3% is recommended, however, more detailed experimental investigations are still necessary to validate this.

6. Conclusions

This study presents the development of translucent and photo-catalytic concrete tiles based on consumer packaging waste glass in different particle size fractions. Based on the presented results, the following conclusions can be drawn:

- In order to secure a proper setting time and strength development of concrete, it is inevitable to apply a washing step to the glass, as the polluted material significantly distorts the hydration of cement, water demand, setting time and mechanical properties of the hardened concrete;
- Concrete mixtures were developed with up to 60 vol% of fine and coarse washed waste glass aggregates;
- ASR can be suppressed in concrete with glass by additions of fly ash or ground granulated blast-furnace slag;
- The translucency of concrete tiles depends on the maximum glass particle size and tile thickness. In order to secure translucent tiles of higher thicknesses, the maximum glass particle size should be respectively larger;
- Exposed glass particles contribute to a better activation of the TiO$_2$ photocatalyst and in turn to a better photocatalytic oxidation efficiency of air pollutants.

Acknowledgements

References

[1] N. Randl, T. Steiner, S. Ofner, E. Baumgartner, T. Mészöly, Development of UHPC mixtures from an ecological point of view, Constr. Build. Mater. 67 (2014) 373–378.
[2] S. Lofti, J. Deja, P. Rem, R. Mróz, E. van Roekel, H. van der Stelt, Mechanical recycling of EOL concrete into high-grade aggregates, Resour. Conserv. Recycl. 87 (2014) 117–125.
[3] S. Lofti, M. Eggimann, E. Wagner, R. Mróz, J. Deja, Performance of recycled aggregate concrete based on a new concrete recycling technology, Constr. Build. Mater. 95 (2015) 243–256.
[4] T.C. Ling, C.S. Poon, Properties of architectural mortar prepared with recycled glass with different particle sizes, Mater. Des. 32 (2011) 2675–2684.
[5] The European Container Glass Federation (FEVE) – Recycling Statistics, 2012.
[6] N. Phonphuak, S. Kanyakam, P. Chindaprasirt, Utilization of waste glass to enhance physical-mechanical properties of fired clay brick, J. Cleaner Prod. 112 (2016) 3057–3062.
[7] T-Ch Ling, Ch-S. Poon, Use of recycled CRT funnel glass as fine aggregate in dry-mixed concrete paving blocks, J. Cleaner Prod. 68 (2014) 209–215.
[8] M.M. Disfani, A. Arulrajah, M.W. Bo, N. Sivakugan, Environmental risks of using recycled crushed glass in road applications, J. Cleaner Prod. 20 (2012) 170–179.
[9] Q.L. Yu, P. Spiesz, H.J.H. Brouwers, Development of cement-based lightweight composites – Part 1: mix design methodology and hardened properties, Cem. Concr. Compos. 44 (2013) 17–29.
[10] P. Spiesz, Q.L. Yu, H.J.H. Brouwers, Development of cement-based lightweight composites – Part 2: durability-related properties, Cem. Concr. Compos. 44 (2013) 30–40.
[11] R. Yu, D.V. van Onna, P. Spiesz, H.J.H. Brouwers, Development of ultra-lightweight fibre reinforced concrete applying expanded waste glass, J. Cleaner Prod. 112 (2016) 690–701.
[12] Q.L. Yu, P. Spiesz, H.J.H. Brouwers, Ultra-lightweight concrete: conceptual design and performance evaluation, Cem. Concr. Compos. 61 (2015) 18–28.
[13] C. Shi, K. Zheng, A review on the use of waste glasses in the production of cement and concrete, Resour. Conserv. Recycl. 52 (2007) 234–247.
[14] J. Deja, Ł. Gołek, Ł. Kołodziej, Application of glass cullet in binder production, Cem. Wapno Beton 6 (2011) 349–354.
[15] C. Shi, Y. Wu, C. Riefler, H. Wang, Characteristics and pozzolanic reactivity of glass powders, Cem. Concr. Res. 35 (2005) 987–993.
[16] A. Shayan, A. Xu, Performance of glass powder as a pozzolanic materials in concrete: a field trial on concrete slabs, Cem. Concr. Res. 36 (2006) 457–468.
[17] G. Chen, H. Lee, K.L. Young, P.L. Yue, A. Wong, T. Tao, K.K. Choi, Glass recycling in cement production – an innovative approach, Waste Manage. 22 (2002) 747–753.

[18] J. Refined, Development of non-traditional glass markets, Resour. Recycl. (1991) 18–21.
[19] J. Uchiyama, Long-term utilization of the glass reasphalt pavement, Pavement (1998) 3–89.
[20] T.C. Ling, C.S. Poon, S.C. Kou, Feasibility of using recycled glass in architectural cement mortars, Cem. Concr. Compos. 33 (2011) 848–854.
[21] Y. Shao, T. Lefort, S. Moras, D. Rodriguez, Studies on concrete containing ground waste glass, Cem. Concr. Res. 30 (2000) 91–100.
[22] S.B. Park, B.C. Lee, Studies on expansion properties in mortar containing waste glass and fibers, Cem. Concr. Res. 34 (2004) 1145–1152.
[23] H. Du, K.-H. Tan, Use of waste glass as sand in mortar: Part 2- alkali-silica reaction and mitigation methods, Cem. Concr. Compos. 35 (2013) 118–126.
[24] M. Thomas, A. Dunster, P. Nixon, B. Blackwell, Effect of fly ash on the expansion of concrete due to alkali-silica reaction – exposure site studies, Cem. Concr. Compos. 33 (2011) 359–367.
[25] M. Thomas, The effect of supplementary cementing materials on alkali-silica reaction: a review, Cem. Concr. Res. 41 (2011) 1224–1231.
[26] B. Taha, G. Nounu, Using lithium nitrate and pozzolanic glass powder in concrete as ASR suppressors, Cem. Concr. Compos. 30 (2008) 497–505.
[27] T. Ichikawa, Alkali-silica reaction, pessimum effects and pozzolanic effect, Cem. Concr. Res. 39 (2009) 716–726.
[28] K.E. Kurtis, G.S. Willis, J.H. Ideker, C.L. Collins, Examination of the effects of LiOH, LiCl and LiNO$_3$ on alkali-silica reaction, Cem. Concr. Res. 34 (2004) 1403–1415.
[29] P.J.M. Monteiro, L. Turanli, F. Bektas, Use of perlite powder to suppress the alkali-silica reaction, Cem. Concr. Res. 35 (2005) 2014–2017.
[30] T. Ramlochan, M. Thomas, K.A. Gruber, The effect of metakaolin on alkali-silica reaction in concrete, Cem. Concr. Res. 30 (2000) 339–344.
[31] M.D.A. Thomas, M.H. Shehata, Use of ternary blends containing silica fume and fly ash to suppress expansion due to alkali-silica reaction in concrete, Cem. Concr. Res. 32 (2002) 341–349.
[32] V. Corinaldesi, G. Gnappi, G. Moriconi, A. Montenero, Reuse of ground waste glass as aggregate for mortars, Waste Manage. 25 (2) (2005) 197–201.
[33] A. Shayan, A. Xu, Value-added utilization of waste glass in concrete, Cem. Concr. Res. 34 (2004) 81–89.
[34] V. Vaitkevičius, E. Šerelis, H. Hilbig, The effect of glass powder on the microstructure of ultra high performance concrete, Constr. Build. Mater. 68 (2014) 102–109.
[35] A. Omran, A. Tagnit-Hamou, Performance of glass-powder concrete in field applications, Constr. Build. Mater. 109 (2016) 84–95.
[36] W. Jin, C. Meyer, S. Baxter, Glascrete – concrete with glass aggregates, ACI Mater. J. 97 (2) (2000) 208–213.
[37] Z.P. Bazant, G. Zi, C. Meyer, Fracture mechanics of ASR in concretes with waste glass particles of different sizes, J. Eng. Mech. 126 (3) (2000) 226–232.
[38] T.-Ch Ling, Ch.-S Poon, A comparative study on the feasible use of recycled beverage and CRT funnel glass as fine aggregate in concrete, J. Cleaner Prod. 29–30 (2012) 46–52.
[39] E.A. Hashmi Al, Z.Z. Ismail, Recycling of waste glass as a partial replacement for fine aggregate in concrete, Waste Manage. 29 (2009) 655–659.
[40] I.B. Topcu, M. Canbaz, Properties of concrete containing waste glass, Cem. Concr. Res. 34 (2) (2004) 267–274.
[41] M.C. Limbachiya, Bulk engineering and durability properties of washed glass sand concrete, Constr. Build. Mater. 23 (2009) 1078–1083.
[42] S.B. Park, B.C. Lee, H.J. Kim, Studies on mechanical properties of concrete containing waste glass aggregate, Cem. Concr. Res. 34 (2004) 2181–2189.
[43] S.C. Kou, C.S. Poon, Properties of self-compacting concrete prepared with recycled glass aggregate, Cem. Concr. Compos. 31 (2009) 107–113.
[44] K. Afshinnia, Rangaraju P. Rao, Impact of combined use of ground glass powder and crushed glass aggregate on selected properties of Portland cement concrete, Constr. Build. Mater. 117 (2016) 263–272.
[45] M.M. Ballari, H.J.H. Brouwers, Full scale demonstration of air-purifying pavement, J. Hazard. Mater. 254–255 (2013) 406–414.
[46] C.S. Poon, E. Cheung, NO removal efficiency of photocatalytic paving blocks prepared with recycled materials, Constr. Build. Mater. 21 (2007) 1746–1753.
[47] J. Chen, C.S. Poon, Photocatalytic activity of titanium dioxide modified concrete materials – influence of utilizing recycled glass cullets as aggregates, J. Environ. Manage. 90 (2009) 3436–3442.
[48] NEN-EN 196-1, Methods of testing cement – Part 1: determination of strength, CEN European Committee for Standardization and Dutch Normalization-Institute, 2005.
[49] ASTM C1260-01, Standard Test Method for Potential Alkali Reactivity of Aggregates (Mortar-Bar Method).
[50] RILEM Recommendation TC, 106-AAR: International assessment of aggregates for alkali-aggregate reactivity, Mater. Struct. 33 (2000) 88–93.
[51] ISO 22197-1, Fine Ceramics (Advanced Ceramics, Advanced Technical Ceramics) – Test Method for Air Purification Performance of Semiconducting Photocatalytic Materials – Part 1: Removal of Nitric Oxide, 2007.
[52] Q.L. Yu, H.J.H. Brouwers, Indoor air purification using heterogeneous photocatalytic oxidation. Part I: experimental study, Appl. Catal. B 92 (2009) 454–461.
[53] G. Hüsken, H.J.H. Brouwers, A new mix design concept for earth-moist concrete: a theoretical and experimental study, Cem. Concr. Res. 38 (2008) 1246–1259.
[54] H.J.H. Brouwers, H.J. Radix, Self-compacting concrete: theoretical and experimental study, Cem. Concr. Res. 35 (2005) 2116–2136.
[55] M. Hunger, An Integral Design Concept for Ecological Self-compacting Concrete (Ph.D thesis), Eindhoven University of Technology, 2010.
[56] G. Quercia, P. Spiesz, G. Hüsken, H.J.H. Brouwers, SCC modification by use of amorphous nano-silica, Cem. Concr. Compos. 45 (2014) 69–81.
[57] G. Hüsken, H.J.H. Brouwers, On the early-age behavior of zero-slump concrete, Cem. Concr. Res. 42 (2012) 401–510.
[58] R. Yu, P. Spiesz, H.J.H. Brouwers, Mix design and properties assessment of Ultra-High Performance Fibre Reinforced Concrete (UHPFRC), Cem. Concr. Res. 56 (2014) 29–39.
[59] R. Yu, P. Spiesz, H.J.H. Brouwers, Effect of nano-silica on the hydration and microstructure development of Ultra-High Performance Concrete (UHPC) with a low binder amount, Constr. Build. Mater. 65 (2014) 140–150.
[60] Q.L. Yu, H.J.H. Brouwers, Design of a novel calcium sulfate-based lightweight composite: towards excellent thermal properties, Adv. Mater. Res. 651 (2013) 745–750.
[61] J.E. Funk, D.R. Dinger, Predictive Process Control of Crowded Particulate Suspension, Applied to Ceramic Manufacturing, Kluwer Academic Press, 1994.
[62] BS-EN 1015-3:1999, Methods of test for mortar for masonry, Determination of consistence of fresh mortar (by flow table).
[63] G.J.Z. Xu, D.F. Watt, P.P. Hudec, Effectiveness of mineral admixtures in reducing ASR expansion, Cem. Concr. Res. 25 (1995) 1125–1236.
[64] N. Schwarz, H. Cam, N. Neithalath, Influence of a fine glass powder on the durability characteristics of concrete and its comparison to fly ash, Cem. Concr. Compos. 30 (2008) 486–496.
[65] S. Chatterji, The role of Ca(OH)$_2$ in the breakdown of Portland cement concrete due to alkali–silica reaction, Cem. Concr. Res. 9 (1979) 185–188.
[66] Q.L. Yu, M.M. Ballari, H.J.H. Brouwers, Indoor air purification using heterogeneous photocatalytic oxidation. Part II: kinetic study, Appl. Catal. B 99 (2010) 58–65.